Results in Physics 51 (2023) 106620

Contents lists available at ScienceDirect

Results in Physics

journal homepage: www.elsevier.com/locate/rinp

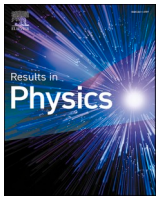

# Optical soliton solutions, bifurcation, and stability analysis of the Chen-Lee-Liu model

S.M. Rayhanul Islam [a], Kamruzzaman Khan [a,b], M. Ali Akbar [c,*]

[a] Department of Mathematics, Pabna University of Science and Technology, Pabna, Bangladesh
[b] School of Science and Technology, University of New England, Armidale, NSW 2351, Australia
[c] Department of Applied Mathematics, University of Rajshahi, Bangladesh

ARTICLE INFO

*Keywords:*
The Chen-Lee-Liu model
Phase plane
Bifurcation
Optical solitons
Solitary waves

ABSTRACT

The Chen-Lee -Liu model has many applications in assorted fields, particularly in the study of nonlinear dynamics, chaos theory, circuit design, signal processing, secure communications, encryption and decryption of chaotic signals, as well as cryptography. The modified extended auxiliary equation mapping method has been applied to the Chen-Lee-Liu model in this article and explores new wave profiles, such as singular periodic solutions, periodic solutions, and kink-type soliton solutions. The complex wave conversion is considered to make a simple differential equation. Three- and two-dimensional images are plotted using Mathematica and MATLAB, and their dispersion and nonlinearity effects are discussed. We also discuss the bifurcation analysis of the studied model. The stability of the equilibrium points is studied, and the phase portrait of the system is presented graphically. The obtained wave profiles might play an important role in telecommunication systems, fiber optics, and nonlinear optics.

## Introduction

The investigation of optical soliton solution (OSS) is the basic fabric of soliton transmission technology in data transmission [1], communications systems [2–4] and optical fibers [5] over the globe. The OSS is an isolated light wave whose form remains unchanged in a wide range, which can produce crystal clear phone calls worldwide [6]. There are a lot of models such as the nonlinear Schrödinger equation [7], the cubic nonlinear Schrödinger equation [8], the complex Ginzburg-Landau equation [9], the Kaup-Newell equation [10] and the Lakshmanan-Posezian-Daniel equation [11,12], the $(2+1)$-dimensional Heisenberg ferromagnetic spin chain equation [13], the $(2+1)$-dimensional Kundu-Mukherjee-Naskar equation [14], that can be described the dynamics of the soliton spectrum in optical fibers, nonlinear optics and metamaterials and so on.

The studied nonlinear Schrödinger (DNLS) equation is a vital nonlinear model in applied science and engineering, such as nonlinear optics, plasma physics, and quantum mechanics. This equation is usually nominated as DNLSE-I, DNLSE-II and DNLSE-III which are instead raised to as the Chen-Lee-Liu (CLL) equation [15], and the Gerjikov-Ivanov equation [16], the higher order nonlinear Schrödinger equation [17] and so on. The wave phenomena of the CLL equation can be used in optical fibers. The signal pulse of the OSS of the CLL equation can be discussed in the optical fiber. Clearly, most of these systems are typically described in the time domain and are described by field propagation at different frequencies. Most dynamic systems have complex partial differential equations and focus on these equations in fiber optic communication systems. In addition, significant advances were made during this period, such as the development of fiber amplifiers, non-linear effects on optical fibers and optical solitons for transmitting data through optical fiber losses. Many scholars have studied the CLL equation and investigated the OSSs. In that sense, Zhang et al. [18] studied the CLL equation through the Darboux transformation that included higher-order components and obtained rogue wave solutions. Yildirim [19] reported the dark, bright, and singular solitons of the CLL equation using the trail equation scheme. Biswas et al. [20] have explored chirped OSSs from the CLL equation by using the extended trial equation scheme. A complex envelope traveling wave method was applied to the CLL equation and explored chirped OSSs by Triki et al. [21]. Bansal et al. [22] reported the dark, bright type OSSs in the CLL equation using the lie symmetry analysis. Recently, Rehman et al. [23] and Akinyemi et al. [24] investigated the new and explicit OSSs of the CLL equation by utilizing the new extended direct algebraic and generalized

* Corresponding author.
*E-mail address:* ali_math74@yahoo.com (M.A. Akbar).

https://doi.org/10.1016/j.rinp.2023.106620
Received 9 May 2023; Received in revised form 31 May 2023; Accepted 6 June 2023
Available online 10 June 2023

$(G'/G)$-expansion approaches. Inc et al. [25] reported the combined optical solitary waves and conservation laws of the CLL equation through complex envelope function ansatz. Ozdemir et al. [26] have investigated OSSs including dark, singular, dark-singular soliton, singular periodic waves and rational function solutions to the perturbed Chen-Lee-Liu equation using the modified extended tanh expansion scheme. Younis et al. [27] have extracted OSSs from the CLL equation through the Fan-extended sub-equation method. The researchers reported some novel OSSs, such as dark and bright singular-type soliton solutions, according to the above discussion in the previous literature.

Stability and bifurcation analysis plays a significant role in understanding the behaviour of dynamic systems. Stability analysis provides a fundamental framework for studying complex phenomena and dynamics in various scientific disciplines, such as physics, reaction diffusions, chemical reactions, biology, engineering, economics, and many other domains. It also helps to predict the long-term behaviour of dynamical systems; in engineering disciplines, it aids in the design and optimization of stable and robust systems, such as electrical circuits, mechanical structures, and chemical processes. Stability analysis is particularly essential in designing and controlling systems to ensure their stability and prevent unwanted behaviours such as oscillations, instabilities, or chaotic dynamics. Bifurcation analysis, on the other hand, explores the qualitative changes that occur in a system as a parameter is varied. It helps uncover critical values of parameters at which the system undergoes transitions, such as the emergence of new equilibrium points or the onset of complex dynamics like chaos. By studying stability and bifurcations, researchers gain valuable insights into the behaviour and stability of dynamical models, enabling a deeper understanding of complex systems in various scientific disciplines.

The MEAEM method has been employed by diverse researchers in various studies for different objectives. Seadawy and Cheema [28] focused on the analysis of the higher-order dispersive extended nonlinear Schrödinger equation using the MEAEM method. Another study by Seadawy et al. [29] examined the application of the MEAEM method in solving time fractional nonlinear evolution equations. Furthermore, Cheemaa et al. [30] applied the MEAEM method to study the Maccari system.

This study aims to establish some inclusive general OSSs through the MEAEM scheme, such as singular periodic solutions, periodic solutions, and kink-type soliton solutions of the CLL model. The wave solutions discussed in this research paper hold great significance in various scientific domains such as optical fibers, nonlinear optics, and communication systems. Additionally, we delve into a detailed examination of the model's stability and conduct a bifurcation analysis to gain a more profound understanding of complex systems in diverse scientific fields.

### *The mathematical model*

The CLL equation was first introduced by Chen et al. [15]:

$$i\frac{\partial \Phi}{\partial t}+\gamma\frac{\partial^2 \Phi}{\partial x^2}+i\mu|\Phi|^2\frac{\partial \Phi}{\partial x}=0 \tag{1.1}$$

where the function $\Phi(x,t)$ represents the complex wave envelopes and where $x$ and $t$ respectively indicate the wave's distance travelled and the time it took to travel that distance. If we choose $\gamma=\mu=1$, the CLL equation is collapsed [21]. In Eq. (1.1), the constant $\gamma$ represents the group velocity dispersion, $\mu$ represents the nonlinear dispersion. Chen et al. [15] used the inverse scattering technique to linearize the nonlinear Hamiltonian system and used part of the Lax equation to test the integrability of the nonlinear Hamiltonian systems. Both of these processes were carried out to determine whether or not the nonlinear Hamiltonian systems were integrable.

The remaining parts of the manuscript are structured as follows: the modified extended auxiliary equation mapping (MEAEM) technique has been deliberated in section 2. The optical soliton and its physical behaviours have in section 3. The stability analysis of the CLL model has been discussed in section 4, and lastly, the conclusion is specified in section 5.

## Overview of the MEAEM method

We will explain the suggested MEAEM approach for studying the optical soliton solution of NLEEs in this section. The NLEEs are considered as the following form:

$$\mho(u,u_t,u_x,u_{xx},u_{tt},u_{xt},\cdots)=0 \tag{2.1}$$

in which $u=u(x,t)$ is a wave function.

**Step 1**: The traveling wave transformation is considered as follows:

$$u(x,t)=u(\xi) \text{ and } \xi=x-\omega t \tag{2.2}$$

In Eq. (2.2), $\omega$ is the wave speed. We obtain the following equation:

$$\mathscr{K}(u,u',u'',u''',\cdots)=0, \tag{2.3}$$

**Step 2.** In the realms of mathematics and physics, an ansatz is a well-informed conjecture that aids in problem-solving and is subsequently verified through its results as part of the solution. When employing the direct method to obtain wave solutions, the selection of an appropriate ansatz holds immense importance. Any individual capable of conceiving a suitable ansatz can discover the desired solution with reduced effort and potentially uncover novel results. In the MEAEM method, an "Ansatz" has been utilized, and it has been established that this particular conjecture is a significant technique. In comparison to other approaches, the MEAEM method offers closed-form wave solutions with a lower number of free parameters for nonlinear evolution equations (NLEEs) than other methods. Consequently, the obtained solutions can effectively explain the observed facts.

We hypothesize that the solution to Equation (2.3) is:

$$u(x,t)=\sum_{j=0}^{m}A_i\Phi^j(\xi)+\sum_{j=-1}^{-m}B_{-j}\Phi^j(\xi)+\sum_{j=2}^{m}C_j\Phi^{j-2}(\xi)\Phi'(\xi)+\sum_{j=1}^{m}C_j\left(\frac{\Phi'(\xi)}{\Phi(\xi)}\right)^j, \tag{2.4}$$

where the constants $A_l, B_l, C_l$, and $D_l$ $(l=0,1,..,m)$ are determined later, the auxiliary equation satisfy to the values of $\Phi(\xi)$ and its derivative $\Phi'(\xi)$.

$$\begin{cases} (\Phi'(\xi))^2=\lambda_1\Phi^2(\xi)+\lambda_2\Phi^3(\xi)+\lambda_3\Phi^4(\xi); \\ \Phi''(\xi)=\lambda_1\Phi(\xi)+\frac{3}{2}\lambda_2\Phi^2(\xi)+2\lambda_3\Phi^3(\xi); \\ \Phi'''(\xi)=\left(\lambda_1+3\lambda_2\Phi(\xi)+6\lambda_3\Phi^2(\xi)\right)\Phi'(\xi); \\ \Phi''''(\xi)=\frac{1}{2}\Phi(\xi)\left(2\lambda_1^2+15\lambda_1\lambda_2\Phi(\xi)+5\left(3\lambda_2^2+8\lambda_1\lambda_2\right)\Phi^2(\xi)+60\lambda_2\lambda_3\Phi^3(\xi)+48\lambda_3^2\Phi'(\xi)\right); \end{cases} \tag{2.5}$$

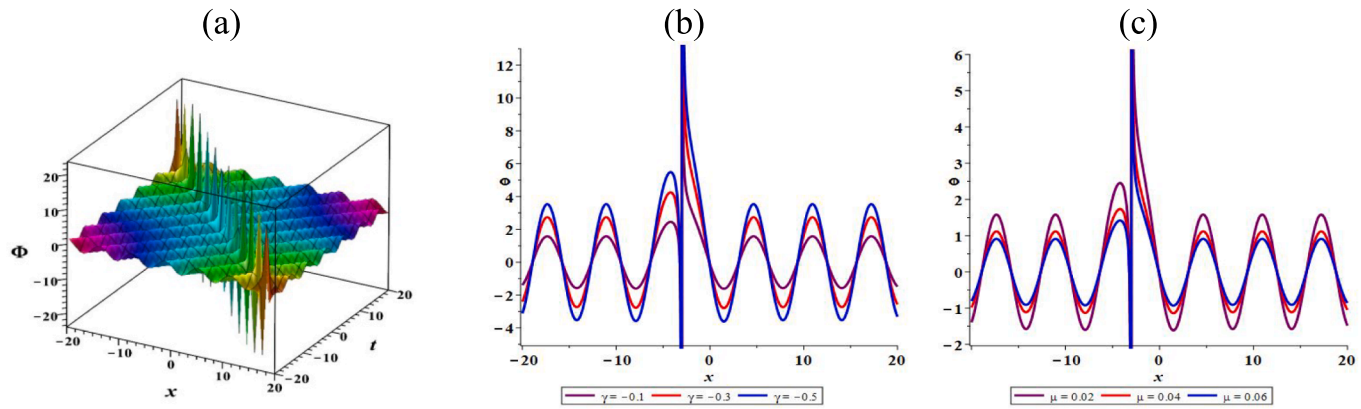


**Fig. 1.** (a) Graphical representation of the solution $|\Phi_1(x,t)|$, (b) Effect of dispersion for $\gamma = -0.1, -0.3, -0.5$ and (c) Effect of nonlinearity $\mu = 0.02, 0.04, 0.06$ at $t = 1.5$.

where $\lambda_1, \lambda_2, \lambda_3 \in R$ and $\lambda_3 \neq 0$.

**Step 3.** To determine the value of $m$ we need to balance between the highest-order non-linear term and the highest-order linear term in Eq. (2.3).

**Step 4.** After inserting Eq. (2.5) into Eq. (2.4) and setting the coefficients of $\Phi'^{\,l}(\xi)\Phi^j(\xi)$ $(l = 0,\ 1;\ j = 1,\ 2,\ 3, \ldots, m)$ to zero, we obtain a system of algebraic equations. By solving this system of equations using Maple 20, the constants $A_l, B_l, C_l$, and $D_l$ $(l = 0, 1, .., m)$ can be determined.

**Step 5.** By entering the values of constants and $\Phi(\xi)$ into Eq. (2.3), and we can derive the necessary solutions from Eq. (2.1) [28,29].

### Optical solitons and their physical behaviours

To use the CLL model to study the importance of OSSs, the following wave conversion is used:

$$\Phi(x,t) = \wp(\xi)\exp(i\phi(x,t)), \tag{3.1}$$

where $\wp(\xi)$ represent the amplitude of the wave as $\xi = x - \omega t$ and $\phi(x,t)$ represents the phase component of the wave as $\phi(x,t) = -\alpha x + \beta t + \theta$. Here, $\omega$ is the traveling wave, $\alpha$ is the frequency of the soliton, $\beta$ is the wave number and $\theta$ is the extra phase component of the soliton depending on $\xi$. By utilizing the wave conversation technique and inserting Equation (3.1) into Equation (1.1), we derived the nonlinear equation and subsequently separated the real and imaginary parts [20]. as:

$$\gamma\wp'' - (\gamma\alpha^2 + \beta)\wp + \mu\alpha\wp^3 = 0, \tag{3.2}$$

and

$$\omega = -2\alpha\gamma + \mu\wp^2, \tag{3.3}$$

The speed of the OSSs is derived from the imaginary component (3.3), whereas the profile of the OSSs is bestowed with the assistance of incorporating the real component (3.2) [20]. Using the balance principle in Eq. (3.2) yields $m = 1$. Now for $m = 1$, Eq. (2.4) takes the following form:

$$\wp(x,t) = A_0 + A_1\Phi(\xi) + \frac{B_1}{\Phi(\xi)} + C_1\frac{\Phi'(\xi)}{\Phi(\xi)}, \tag{3.4}$$

Putting Eq. (2.5) and solution (3.4) into Eq. (3.2), and collecting all terms in the same order of $\Phi'^{\,l}(\xi)\Phi^j(\xi)$ $(l = 0,\ 1;\ j = 1,\ 2,\ 3, \ldots, m)$, we get the system of algebraic equations and solving them, yields a solution set.

$$\beta = -\frac{\gamma(2\alpha^2 + \lambda_1)}{2}, A_0 = 0, A_1 = \pm\sqrt{-\frac{\lambda_3\gamma}{2\alpha\mu}}, B_1 = 0, C_1 = \pm\sqrt{-\frac{\gamma}{2\alpha\mu}} \tag{3.5}$$

Substituting the positive values from (3.5) in solution (3.4), the optical soliton solutions of Eq. (1.1) are obtained as:

$$\Phi_1(x,t) = -\frac{\lambda_1\sqrt{-\frac{2\lambda_3\gamma}{\alpha\mu}}\left(\epsilon\coth\left(\frac{M}{2}\right) + 1\right)}{4\sqrt{\lambda_1\lambda_3}} + \frac{\epsilon\sqrt{\lambda_1}\sqrt{-\frac{2\gamma}{\alpha\mu}}\left(1 - \coth^2\left(\frac{M}{2}\right)\right)}{4\left(\epsilon\coth\left(\frac{M}{2}\right) + 1\right)} \times e^{i(-\alpha x + \beta t + \theta)} \tag{3.6}$$

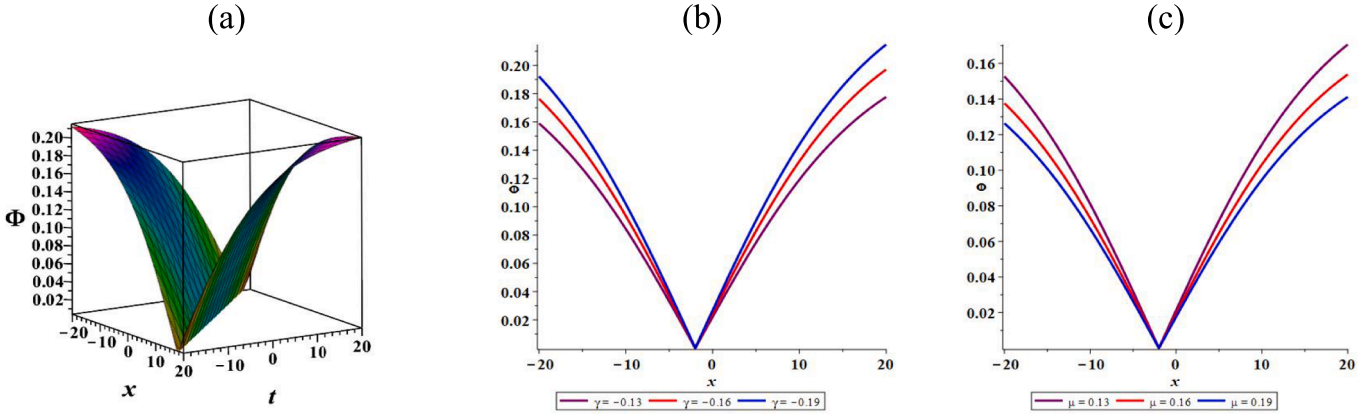


**Fig. 2.** (a) Graphical representation of the solution $|\Phi_2(x,t)|$, (b) Effect of dispersion for $\gamma = -0.13, -0.16, -0.19$, and (c) Effect of nonlinearity $\mu = 0.13, 0.16, 0.19$ at $t = 1.5$.

where $\lambda_1 > 0, \epsilon = \pm 1, \lambda_2^2 - 4\lambda_1\lambda_3 = 0$, $\beta = -\frac{\gamma(2\alpha^2+\lambda_1)}{2}, M = \sqrt{\lambda_1}(\xi + v_0)$ and $\xi = x - \omega t$. Now, if we set $\alpha = 1, \mu = 0.02, \gamma = -0.1, \lambda_1 = 1, \lambda_3 = 2.3, \omega = -1, v_0 = 1.5, \epsilon = 1, \beta = 0.15, \theta = 0$ in Eq. (3.6), we get the singular periodic solution of $|\Phi_1(x,t)|$ as displayed in Fig. 1(a). Fig. 1(b) and (c) signify the 2D line chart of the same solution, which is displayed the dispersion and nonlinearity effects.

$$\Phi_2(x,t) = \left( -\frac{\sqrt{\frac{\lambda_1}{\lambda_3}}\sqrt{-\frac{2\lambda_3\gamma}{\alpha\mu}}\left(\frac{\epsilon sinh(M)}{\cosh(M)+\eta}+1\right)}{4} + \frac{\sqrt{-\frac{2\gamma}{\alpha\mu}}\left(\frac{\epsilon\sqrt{\lambda_1}\cosh(M)}{\cosh(M)+\eta} - \frac{\epsilon\sqrt{\lambda_1}\,sinh^2(M)}{(\cosh(M)+\eta)^2}\right)}{2\left(\frac{\epsilon sinh(M)}{\cosh(M)+\eta}+1\right)} \right) \times e^{i(-\alpha x+\beta t+\theta)} \tag{3.7}$$

where $\lambda_1, \lambda_3 > 0, (\epsilon, \eta) = (1,1), (1,-1), (-1,1), (-1,-1), \lambda_2^2 - 4\lambda_1\lambda_3 = 0, M = \sqrt{\lambda_1}(\xi + v_0), \beta = -\frac{\gamma(2\alpha^2+\lambda_1)}{2}$ and $\xi = x - \omega t$. The 3D and 2D line plots of Eq. (3.7) are given as:

The 3D plot of the solution $|\Phi_2(x,t)|$ signifies the $v$-shape structure for choosing the values of the parameters $\alpha = 0.11, \mu = 0.12, \gamma = 0.13, \lambda_1 = 0.01, \lambda_3 = 0.1, \omega = -1, v_0 = 2, \epsilon = 1, \beta = 0.13, \theta = 0, \eta = 1$, which are displayed in Fig. 2(a). Such behavior is confirmed by their 2D line plot at $t = 1.5$ as shown in Fig. 2(b) and Fig. 2(c) respectively. It further notes that Fig. 2(b) represents the dispersion effect and the nonlinearity effect is represented in Fig. 2(c).

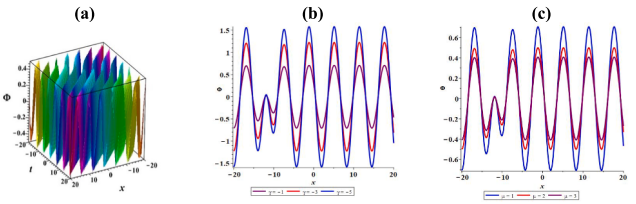


**Fig. 3.** (a) Graphical representation of the real part of the solution $\Phi_3(x,t)$, (b) Effect of dispersion for $= -1, -3, -5$, and (c) Effect of nonlinearity $\mu = 1, 2, 3$ at $t = 1.5$.

$1, p = 0.1$. The 2D line plot of such types of wave profiles is represented in Fig. 3(b) and (c), which are shown in the dispersion and nonlinearity effects of the CLL model.

Fig. 4(a) represents the kink-type structure of $|\Phi_3(x,t)|$ for choosing the parameters $\alpha = 0.01, \mu = 0.3, \gamma = 0.13, \lambda_1 = 0.01, \lambda_3 = 0.2, \omega = -1, v_0 = 12, \epsilon = -1, \beta = 0.3, \theta = 0.2, \eta = 1, p = 0.1$. Such types of wave profiles are explored in 2D line plots of the same solutions as represented in Fig. 4(b) and (c), which are revealed in the dispersion and nonlinearity effects of the CLL model.

Substituting the negative values from (3.5) in solution (3.4), the attain the results of Eq. (1.1) are

$$\Phi_3(x,t) = \left( -\frac{\lambda_1\sqrt{-\frac{2\lambda_3\gamma}{\alpha\mu}}\left(\frac{\epsilon(sinh(M)+p)}{\cosh(M)+\eta\sqrt{p^2+1}}+1\right)}{4\sqrt{\lambda_1\lambda_3}} + \frac{\sqrt{-\frac{2\gamma}{\alpha\mu}}\left(\frac{\epsilon\sqrt{\lambda_1}\cosh(M)}{\cosh(M)+\eta\sqrt{p^2+1}} - \frac{\epsilon(\sinh(M)+p)\sqrt{\lambda_1}\sinh(M)}{\left(\cosh(M)+\eta\sqrt{p^2+1}\right)^2}\right)}{2\left(\frac{\epsilon(sinh(M)+p)}{\cosh(M)+\eta\sqrt{p^2+1}}+1\right)} \right) \times e^{i(-\alpha x+\beta t+\theta)} \tag{3.8}$$

where $\lambda_1 > 0, (\epsilon, \eta) = (1,1), (1,-1), (-1,1), (-1,-1), \lambda_2^2 - 4\lambda_1\lambda_3 = 0, M = \sqrt{\lambda_1}(\xi + v_0), \beta = -\frac{\gamma(2\alpha^2+\lambda_1)}{2}$ and $\xi = x - \omega t$. The 3D and 2D line plots of Eq. (3.8) are given as

Fig. 3(a) represents the periodic wave profiles of the solution $\mathrm{Re}(\Phi_3(x,t))$ for selecting the parameters $\alpha = 0.01, \mu = 0.3, \gamma = 0.13, \lambda_1 = 0.01, \lambda_3 = 0.2, \omega = -1, v_0 = 12, \epsilon = -1, \beta = 0.3, \theta = 0.2, \eta =$

$$\Phi_4(x,t) = \frac{\lambda_1\sqrt{-\frac{2\lambda_3\gamma}{\alpha\mu}}\left(\epsilon\coth\left(\frac{M}{2}\right)+1\right)}{4\sqrt{\lambda_1\lambda_3}} + \frac{\epsilon\sqrt{\lambda_1}\sqrt{-\frac{2\gamma}{\alpha\mu}}\left(1-\coth^2\left(\frac{M}{2}\right)\right)}{4\left(\epsilon\coth\left(\frac{M}{2}\right)+1\right)} \times e^{i(-\alpha x+\beta t+\theta)} \tag{3.9}$$

where $\lambda_1 > 0, \epsilon = \pm 1, \lambda_2^2 - 4\lambda_1\lambda_3 = 0, M = \sqrt{\lambda_1}(\xi + v_0), \beta = -\frac{\gamma(2\alpha^2+\lambda_1)}{2}$,

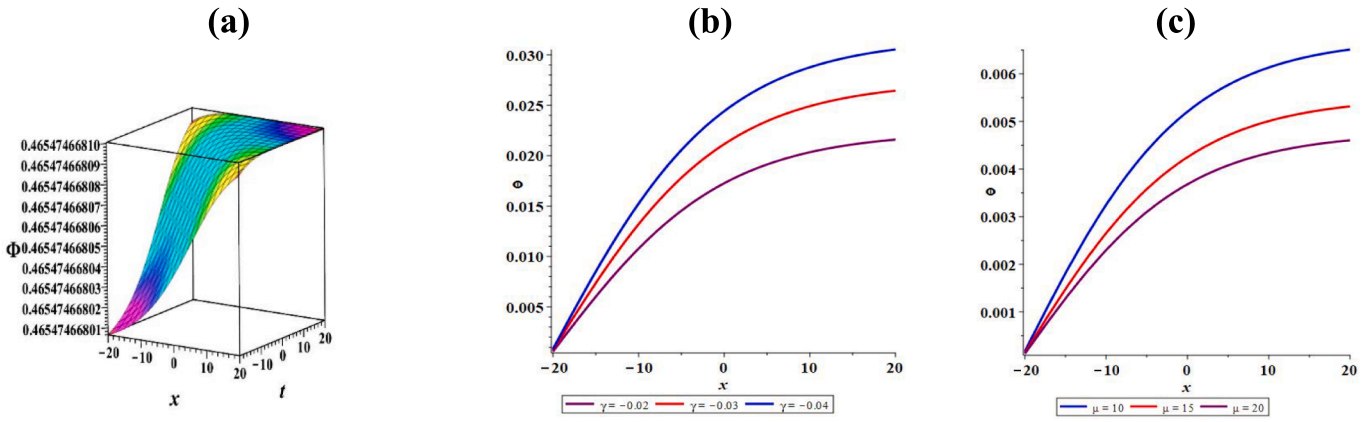


**Fig. 4.** (a) Graphical representation of the solution $|\Phi_3(x,t)|$, (b) Effect of dispersion for $\gamma = -0.02, -0.03, -0.04$, and (c) Effect of nonlinearity $\mu = 10, 15, 20$ at $t = 1.5$.

and $\xi = x - \omega t$.

$$\Phi_5(x,t) = \left( \frac{\sqrt{\frac{\lambda_1}{\lambda_3}}\sqrt{-\frac{2\lambda_3\gamma}{\alpha\mu}}\left(\frac{\epsilon sinh(M)}{\cosh(M)+\eta}+1\right)}{4} - \frac{\sqrt{-\frac{2\gamma}{\alpha\mu}}\left(\frac{\epsilon\sqrt{\lambda_1}\cosh(M)}{\cosh(M)+\eta} - \frac{\epsilon\sqrt{\lambda_1}\sinh^2(M)}{(\cosh(M)+\eta)^2}\right)}{2\left(\frac{\epsilon sinh(M)}{\cosh(M)+\eta}+1\right)} \right) e^{i(-\alpha x+\beta t+\theta)} \tag{3.10}$$

where $\lambda_1, \lambda_3 > 0, (\epsilon, \eta) = (1,1), (1,-1), (-1,1)(-1,-1), \lambda_2^2 - 4\lambda_1\lambda_3 = 0, M = \sqrt{\lambda_1}(\xi + v_0), \beta = -\frac{\gamma(2\alpha^2+\lambda_1)}{2}$ and $\xi = x - \omega t$.

$$\Phi_6(x,t) = \left( \frac{\lambda_1\sqrt{-\frac{2\lambda_3\gamma}{\alpha\mu}}\left(\frac{\epsilon(sinh(M)+p)}{\cosh(M)+\eta\sqrt{p^2+1}}+1\right)}{4\sqrt{\lambda_1\lambda_3}} - \frac{\sqrt{-\frac{2\gamma}{\alpha\mu}}\left(\frac{\epsilon\sqrt{\lambda_1}\cosh(M)}{\cosh(M)+\eta\sqrt{p^2+1}} - \frac{\epsilon(\sinh(M)+p)\sqrt{\lambda_1}\sinh(M)}{\left(\cosh(M)+\eta\sqrt{p^2+1}\right)^2}\right)}{2\left(\frac{\epsilon(sinh(M)+p)}{\cosh(M)+\eta\sqrt{p^2+1}}+1\right)} \right) \times e^{i(-\alpha x+\beta t+\theta)} \tag{3.11}$$

where $\lambda_1 > 0, (\epsilon, \eta) = (1,1), (1,-1), (-1,1), (-1,-1), \lambda_2^2 - 4\lambda_1\lambda_3 = 0$, $\beta = -\frac{\gamma(2\alpha^2+\lambda_1)}{2}$, $M = \sqrt{\lambda_1}(\xi + v_0)$ and $\xi = x - \omega t$. The 3D and 2D line plot of the Eq. (3.11) is given as

The periodic structure of the solution $|\Phi_6(x,t)|$ for choosing the parameters $\alpha = 1, \mu = 0.01, \gamma = 0.02, \lambda_1 = -0.15, \lambda_3 = 1.5, \omega = 1, v_0 = 1, \epsilon = 1, \beta = 1, \theta = 1, \eta = -1, p = 1$, which as shown in Fig. 5(a). Fig. 5(b) and 5(c) also represent the dispersion and the nonlinearity effects of the CLL model.

It is understood from Fig. 1(b)-5(b) that the amplitude of the soliton increases with the increases of $\gamma$. It is also seen in the Fig. 1(c)-5(c) that the amplitude of the soliton decreases with the increases of $\mu$. The attained optical soliton solutions can be more applicable in optical fibers, communication systems, telecommunication systems, nonlinear optics and other domains.

## Stability analysis of the CLL equation

We set $X = u$, $Y = X'$ to start the phase plane analysis for the CLL problem. We can now rewrite Equation (3.2) as a first-order dynamical system using the following notation:

$$\begin{cases} \dfrac{dX}{d\xi} = Y = f(X,Y), \\ \dfrac{dY}{d\xi} = \dfrac{\gamma\alpha^2+\beta}{\gamma}X - \dfrac{\mu\alpha}{\gamma}X^3 = g(X,Y), \end{cases} \tag{4.1}$$

which defines the well-known phase plane associated with optical solutions of the CLL equation. The differential equation Eq. (3.2) or Eq. (4.1) comes from the Hamiltonian

$$H(X,Y) = \frac{Y^2}{2} - \frac{\gamma\alpha^2+\beta}{2\gamma}X^2 + \frac{\mu\alpha}{4\gamma}X^4 \tag{4.2}$$

by using Hamilton canonical equations $X' = \frac{\partial H}{\partial Y}$ and $Y' = \frac{\partial H}{\partial X}$.

If $\beta = -\gamma\alpha^2$, the system has only one equilibrium point as $(X^*, Y^*) = (0,0)$. On the other hand, if $\beta \neq -\gamma\alpha^2$, then the system has three equi-

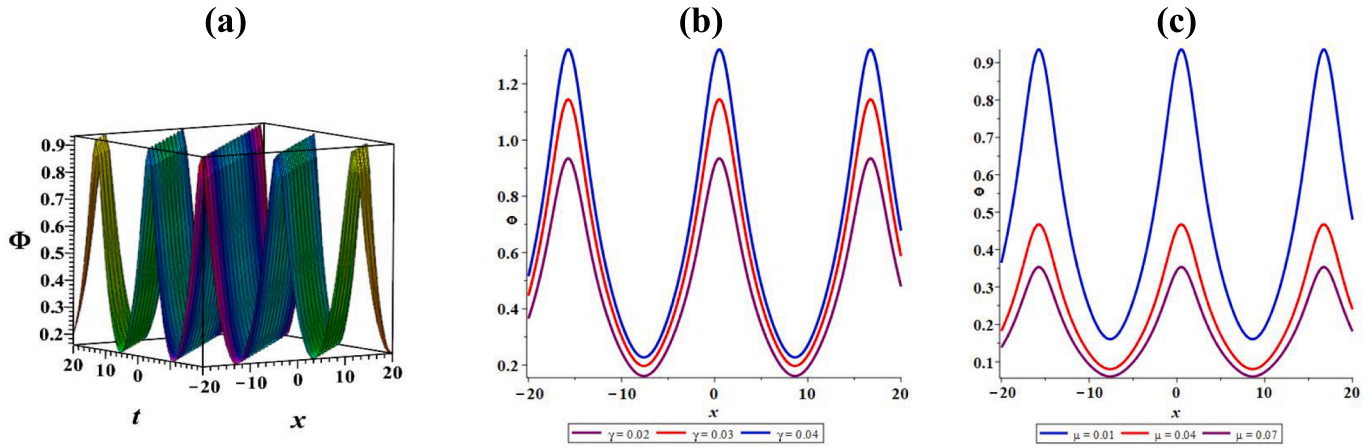


**Fig. 5.** (a) Graphical representation of the solution $|\Phi_6(x,t)|$, (b) Effect of dispersion for $\gamma = 0.02, 0.03, 0.04$, and (c) Effect of nonlinearity $\mu = 0.01, 0.04$ and $0.07$ at $t = 1.5$.

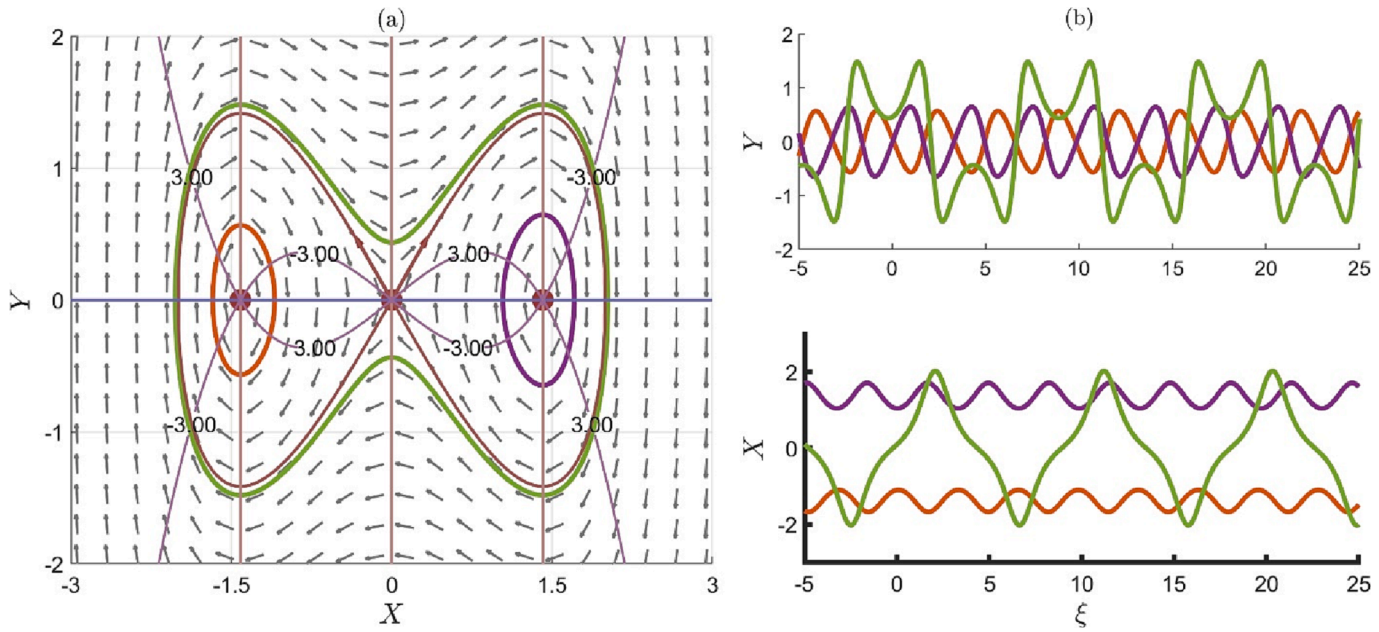


**Fig. 6.** Phase portrait of the planar system (4.1) for the values of $\alpha = 1, \beta = 1, \gamma = 1, \mu = 1$. Fig. 6(a) represents the trajectories of the system along with isoclines and nullclines, and Fig. 6(b) depicted the corresponding solutions of the trajectories in terms of wave variable $\xi$.

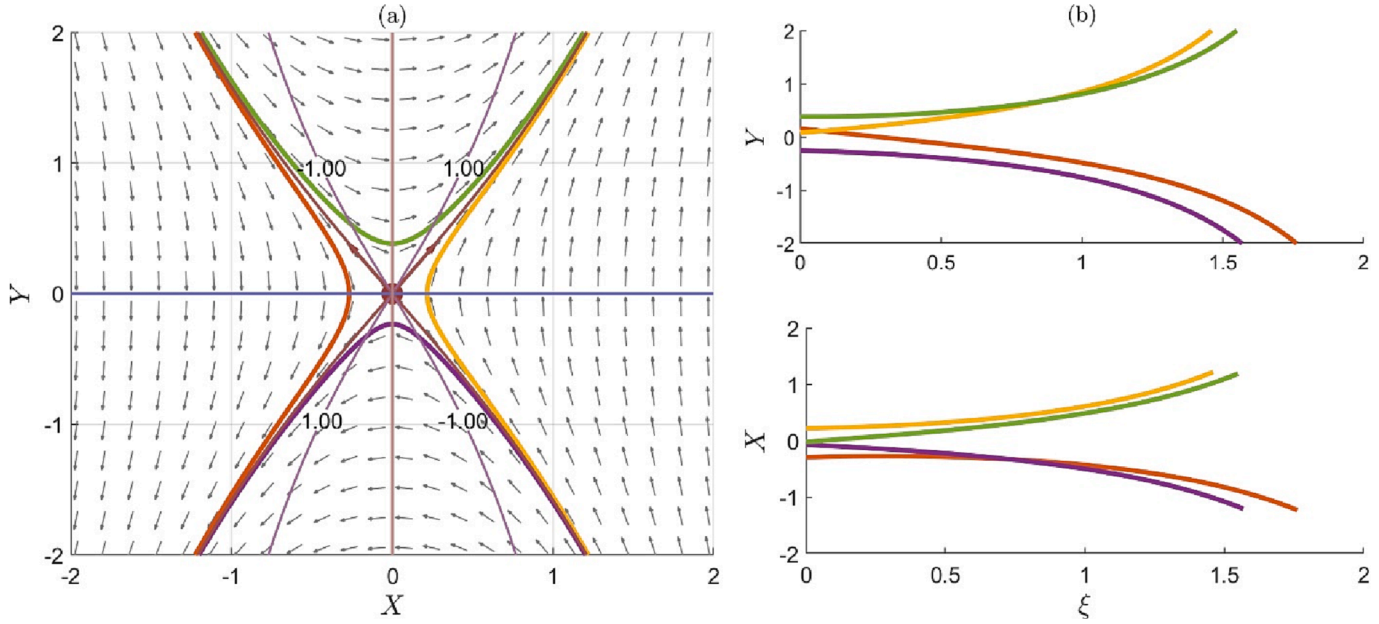


**Fig. 7.** Phase portrait of the planar system (4.1) for the values of $\alpha = 1, \beta = 1, \gamma = 1, \mu = -1$. Fig. 7(a) represents the trajectories of the system along with isoclines and nullclines, and Fig. 7(b) depicted the corresponding solutions of the trajectories in terms of wave variable $\xi$.

libria $(0,0)$, $\left(\sqrt{\frac{\gamma\alpha^2+\beta}{\mu\alpha}}, 0\right)$ and $\left(-\sqrt{\frac{\gamma\alpha^2+\beta}{\mu\alpha}}, 0\right)$. Note that $\mu\alpha \neq 0$.

The Jacobian matrix is $J(X,Y) = \frac{\partial(f,g)}{\partial(X,Y)} = \begin{pmatrix} \frac{\partial f}{\partial X} & \frac{\partial f}{\partial Y} \\ \frac{\partial g}{\partial X} & \frac{\partial g}{\partial Y} \end{pmatrix}_{(X^*,Y^*)} = \begin{pmatrix} 0 & 1 \\ \frac{\gamma\alpha^2+\beta}{\gamma} - \frac{3\mu\alpha}{\gamma}X^2 & 0 \end{pmatrix}$.

The eigenvalues of $J$ are given by $\det(J - \lambda I_{2\times 2}) = 0$ which implies

$\lambda^2 - tr(J)\lambda + \det(J) = 0$

where $tr(J) = 0, \det(J) = \frac{3\mu\alpha}{\gamma}X^2 - \frac{\gamma\alpha^2+\beta}{\gamma}$.

***Case 1**: Stability of the equilibrium point* $(0,0)$

In this case, the eigenvalues are $\lambda_1 = \sqrt{\frac{\gamma\alpha^2+\beta}{\gamma}}$ and $\lambda_2 = -\sqrt{\frac{\gamma\alpha^2+\beta}{\gamma}}$. If $\frac{\gamma\alpha^2+\beta}{\gamma} > 0$, then the eigenvalues $\lambda_1 = \sqrt{\frac{\gamma\alpha^2+\beta}{\gamma}}$ and $\lambda_2 = -\sqrt{\frac{\gamma\alpha^2+\beta}{\gamma}}$ are the real, opposite sign. Therefore, the equilibrium of $(0.0)$ is unstable saddle point (See Figs. 6 and 7). If $\frac{\gamma\alpha^2+\beta}{\gamma} < 0$, then the eigenvalues are $\lambda_1 = i\sqrt{\frac{\gamma\alpha^2+\beta}{\gamma}}$ and $\lambda_2 = -i\sqrt{\frac{\gamma\alpha^2+\beta}{\gamma}}$ (imaginary) and the given equilibrium point is a stable centre or ellipse (See Figs. 8-10). That is, the stability of $(0,0)$

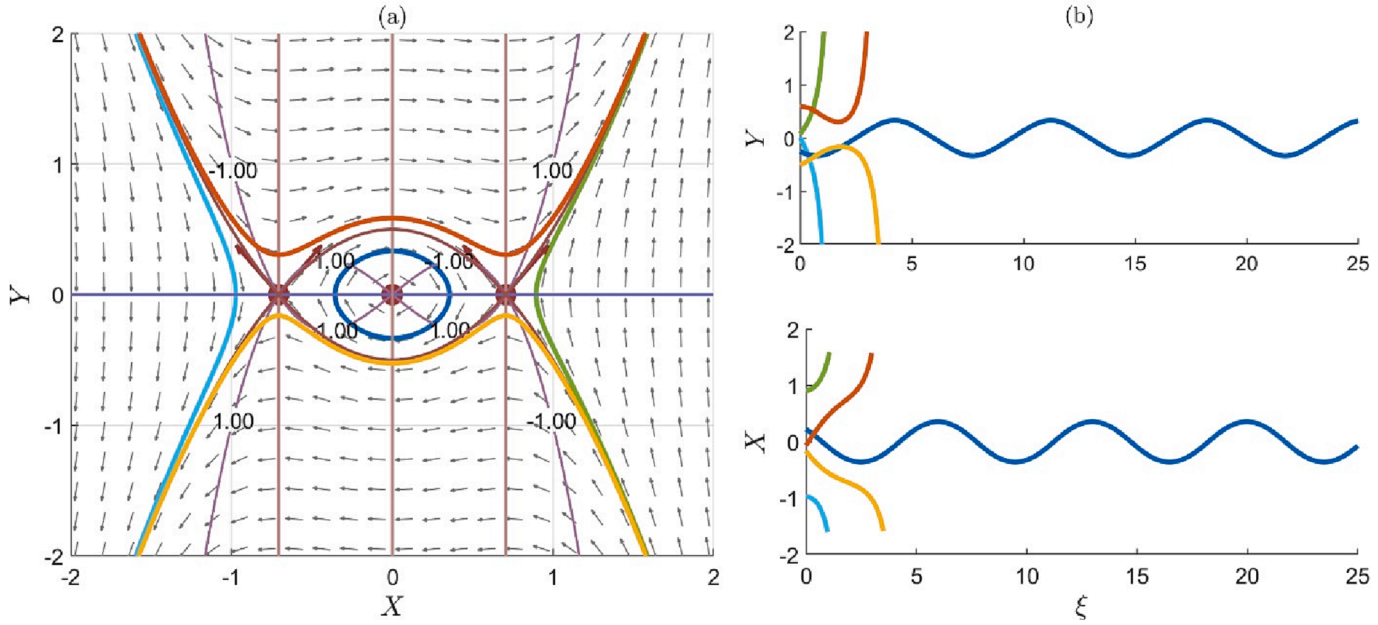


**Fig. 8.** Phase portrait of the planar system (4.1) for the values of $\alpha = -1, \beta = -1, \gamma = 0.5, \mu = 1$. Fig. 8(a) represents the trajectories of the system along with isoclines and nullclines, and Fig. 8(b) depicted the corresponding solutions of the trajectories in terms of wave variable $\xi$.

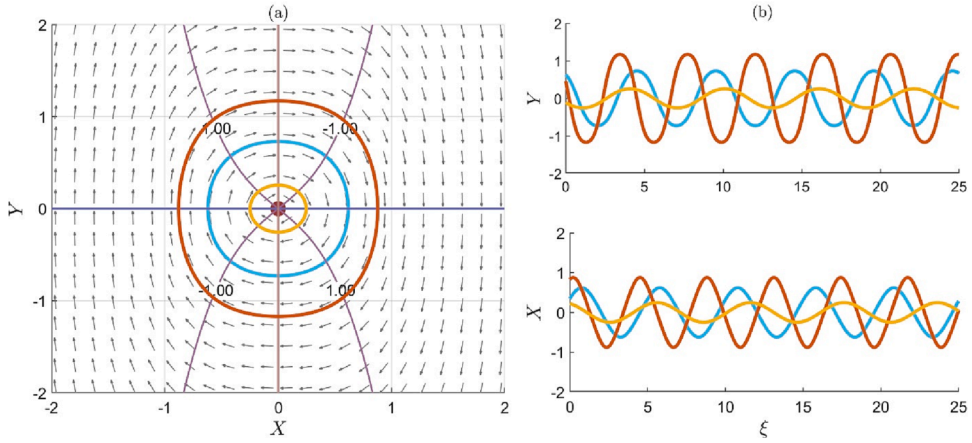


**Fig. 9.** Phase portrait of the planar system (4.1) for the values of $\alpha = -1, \beta = -1, \gamma = 0.5, \mu = -1$. Fig. 9(a) represents the trajectories of the system along with isoclines and nullclines, and Fig. 9(b) depicted the corresponding solutions of the trajectories in terms of wave variable $\xi$.

is altered from an unstable saddle to stable centres due to the change in the values of the parameters.

***Case 2:*** *Stability of the equilibrium points* $\left(\pm\sqrt{\frac{\gamma\alpha^2+\beta}{\mu\alpha}}, 0\right)$

In this case, the characteristic roots are $\lambda_1 = i\sqrt{\frac{2(\gamma\alpha^2+\beta)}{\gamma}}$ and $\lambda_2 = -i\sqrt{\frac{2(\gamma\alpha^2+\beta)}{\gamma}}$. If $\mu\alpha > 0$ and $\frac{\gamma\alpha^2+\beta}{\gamma} > 0$, then the eigenvalues $\lambda_1 = i\sqrt{\frac{2(\gamma\alpha^2+\beta)}{\gamma}}$ and $\lambda_2 = -i\sqrt{\frac{2(\gamma\alpha^2+\beta)}{\gamma}}$ are imaginary, and thus the equilibrium points $\left(\pm\sqrt{\frac{\gamma\alpha^2+\beta}{\mu\alpha}}, 0\right)$ are stable centres (See Fig. 6), whereas for $\mu\alpha > 0$ and $\frac{\gamma\alpha^2+\beta}{\gamma} < 0$, the eigenvalues $\lambda_1 = \sqrt{\frac{2(\gamma\alpha^2+\beta)}{\gamma}}$ and $\lambda_2 = -\sqrt{\frac{2(\gamma\alpha^2+\beta)}{\gamma}}$ are the real, opposite sign. Therefore, the equilibria $\left(\pm\sqrt{\frac{2(\gamma\alpha^2+\beta)}{\gamma}}, 0\right)$ are unstable saddles (See Fig. 8). Analogous to Case 1, the stability of $\left(\pm\sqrt{\frac{\gamma\alpha^2+\beta}{\mu\alpha}}, 0\right)$ are altered from stable centres to unstable saddles due to the change in the values of the parameters.

## Conclusion

The Chen-Lee-Liu model has been examined in this article to reveal important optical soliton solutions. With the help of parameter constraints and a modified extended auxiliary equation mapping method, periodic, singular periodic, and kink-type solutions have been found. These wave profiles have useful applications in nonlinear optics, quantum simulation, high-energy physics, the transmission of light pulses in optical fibers, cosmology, reaction–diffusion wave propagation in near-shore regions, and coastal erosion. The physical conception is explained by drawing two- and three-dimensional diagrams and discussing the dispersion and nonlinearity effects of solutions for different values of the parameters. It is perceived from Figs. 1-5 that the amplitude increases with increasing dispersion coefficient. On the other hand, the amplitude decreases with increasing nonlinear coefficient. We also presented the bifurcation analysis of the studied model. The stability of the equilibrium points is studied, and a phase portrait of the system is presented

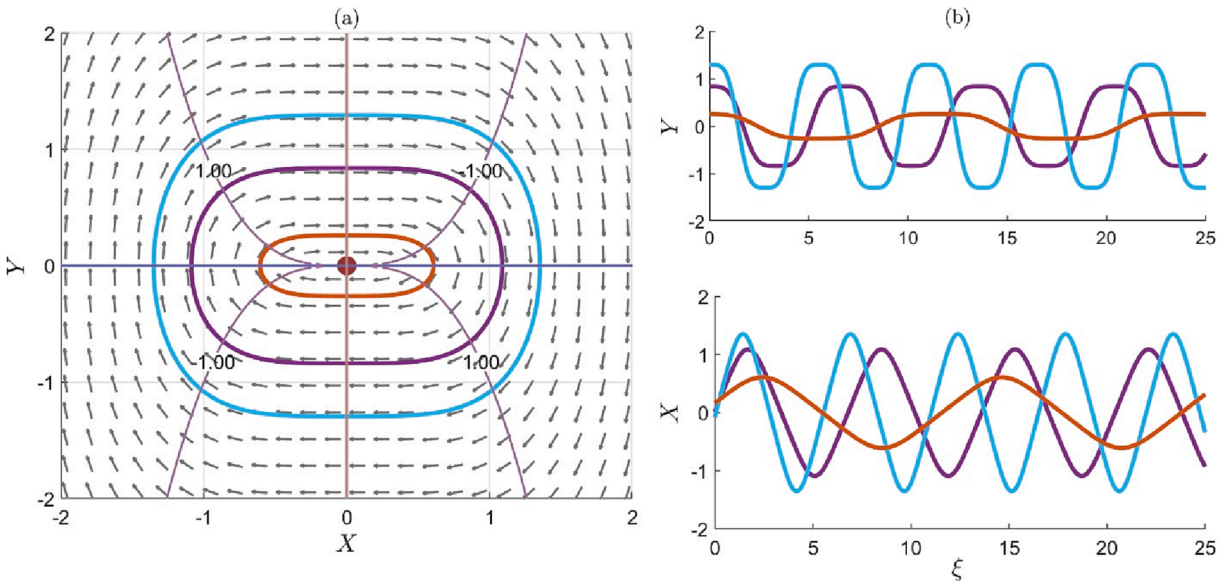


**Fig. 10.** Phase portrait of the planar system (4.1) for the values of $\alpha = -1, \beta = -1, \gamma = 1, \mu = -1$. Fig. 10(a) represents the trajectories of the system along with isoclines and nullclines, and Fig. 10(b) depicted the corresponding solutions of the trajectories in terms of wave variable $\xi$.

graphically in Figs. 6-10. Through bifurcation, from the analysis, we may conclude that the change of the values of the parameters can alter the dynamics of the optical soliton solutions of the Chen-Lee-Liu model and can play an important role in optical fibers, nonlinear optics and communication systems.

## CRediT authorship contribution statement

**S.M. Rayhanul Islam:** Conceptualization, Resources, Methodology, Investigation, Writing – original draft. **Kamruzzaman Khan:** Formal analysis, Software, Visualization, Data curation, Writing – review & editing. **M. Ali Akbar:** Validation, Project administration, Funding acquisition, Supervision.

## Declaration of Competing Interest

The authors declare that they have no known competing financial interests or personal relationships that could have appeared to influence the work reported in this paper.

## Data availability

No data was used for the research described in the article.

## Acknowledgement

The authors would like to express their sincere gratitude to the anonymous reviewer and the editor for providing valuable feedback and suggestions to enhance the quality of the article.

## References

[1] Nakazawa M, Kubota H, Suzuki K, Yamada E, Sahara A. Recent progress in soliton transmission technology. Chaos: J Nonlinear Sci 2000;10(3):486–514.
[2] Bagri M, Kumar S. Solitons transmission system: A dynamic shift in optical fiber communication. Indian J Sci Tech 2020;13:2193–202.
[3] Sadegh AI, Afroozeh A. Introduction of Soliton Generation. Ring Resonator Systems to Perform Optical Communication Enhancement Using Soliton. Springer Briefs in Applied Sciences and Technology. Singapore: Springer; 2015.
[4] Ferreira MF, Facão MV, Latas SV, Sousa MH. Optical solitons in fibers for communication systems. Fiber Integr Opt 2007;24:287–313.
[5] Triki H, Babatin MM, Biswas A. Chirped bright solitons for Chen-Lee-Liu equation in optical fibers and PCF. Optik-Int J Light Electron Opt 2017;149:300–3.
[6] Mollenauer LF, Gordon JP. Solitons in Optical Fibers: Fundamentals and Applications. (New York: Academic; 2006.
[7] Raza N, Zubair A. Bright, dark and dark-singular soliton solutions of nonlinear Schrödinger's equation with spatio-temporal dispersion. J Mod Opt 2018;65:1975–82.
[8] Islam SMR. The traveling wave solutions of the Cubic nonlinear Schrodinger equation using enhanced (G'/G)-expansion method. World Appl Sci J 2015;33:659–67.
[9] Tasbozan O, Kurt A, Tozar A. New optical solutions of complex Ginzburg-Landau equation arising in semiconductor lasers. Appl Phys B 2019;125:104.
[10] Kaup DJ, Newell AC. An exact solution for a derivative nonlinear Schrodinger equation. J Math Phys 1978;19:798–801.
[11] Bansal A, Biswas A, Triki H, Zhou Q, Moshokoa SP, Belic M. Optical solitons and group invariant solutions to Lakshmanan-Porsezian-Daniel model in optical fibers and PCF. Optik 2018;160:86–91.
[12] Ismael HF, Baskonus HM, Bulut H. Abundant novel solutions of the conformable Lakshmanan-Porsezian-Daniel model. Discrete Continuous Dyn Syst S 2021;14:2311–33.
[13] Bashar MH, Islam SMR, Kumar D. Construction of traveling wave solutions of the (2+1)-dimensional Heisenberg ferromagnetic spin chain equation. Partial Differ Equ Appl Math 2021;4:100040.
[14] Islam SMR, Kumar D, Fendzi-Donfack E, Inc M. Impacts of nonlinearity and wave dispersion parameters on the soliton pulses of the (2+1)-dimensional Kundu-Mukherjee-Naskar equation. Rev Mex Fis 2022;68(6):061301.
[15] Chen HH, Lee YC, Liu CS. Integrability of nonlinear Hamiltonian systems by inverse scattering method. Phys Scr 1979;20:490–2.
[16] Gerdjikov VS, Ivanov MI. The quadratic bundle of general form and the nonlinear evolution equations. Expansions over the squared solutions-generalized Fourier transform. Bulg J Phys 1983;10:130–43.
[17] Li Z, Li L, Tian H, Zhou G. New types of solitary wave solutions for the higher order nonlinear Schrödinger equation. Phys Rev Lett 2000;84:4096–9.
[18] Zhang J, Liu W, Qiu D, Zhang Y, Porsezian K, He J. Rogue wave solutions of a higher-order Chen-Lee-Liu equation. Phys Scr 2015;90(5):055207.
[19] Yildirim Y. Optical solitons to Chen-Lee-Liu model with trail equation approach. Optik 2019;183:849–53.
[20] Biswas A, Ekici M, Sonmezoglu A, Alshomrani AS, Zhou Q, Moshokoa SP, et al. Chirped optical solitons of Chen-Lee-Liu equation by extended trial equation scheme. Optik 2018;156:999–1006.
[21] Triki H, Hamaizi Y, Zhou Q, Biswas A, Ullah MZ, Moshokoa SP, et al. Chirped singular solitons for Chen-Lee-Liu equation in optical fibers and PCF. Optik 2018;157:156–60.
[22] Bansal A, Biswas A, Zhou Q, Arshed S, Alzahrani AK, Belic MR. Optical solitons with Chen-Lee-Liu equation by Lie symmetry. Phys Lett A 2020;384(10):126202.
[23] Rehman H, Bibi M, Saleem MS, Rezazadeh H, Adel W. New optical soliton solutions of the Chen-Lee-Liu equation. Int J Mod Phys B 2021;35:2150184.
[24] Akinyemi L, Ullah N, Akbar Y, Hashemi MS, Akbulut A, Rezazadeh H. Explicit solutions to nonlinear Chen-Lee-Liu equation. Mod Phys Lett B 2021;35:2150438.
[25] Inc M, Aliyu AI, Yusuf A, Baleanu D. Combined optical solitary waves and conservation laws for nonlinear Chen-Lee-Liu equation in optical fibers. Optik 2018;158:297–304.
[26] Ozdemir N, Esen H, Secer A, Bayram M, Yusuf A, Sulaiman TA. Optical soliton solutions to Chen-Lee-Liu model by the modified extended tanh expansion scheme. Optik 2021;245:167643.

[27] Younis M, Younas U, Bilal M, Rehman SU, Rizvi STR. Investigation of optical solitons with Chen-Lee-Liu equation of monomode fibers by five free parameters. Indian J Phys 2022;96:1539–46.
[28] Seadawy AR, Cheema N. Applications of extended modified auxiliary equation mapping method for high-order dispersive extended nonlinear Schrodinger equation in nonlinear optics. Mod Phys Lett B 2019;33:1950203.
[29] Seadawy AR, Ali A, Raddadi MH. Exact and solitary wave solutions of conformal time fractional Clannish Random Walker's Parabolic and Ablowitz-Kaup-Newell-Segur equations via modified mathematical methods. Results Phys 2021;26:104374.
[30] Cheemaa N, Chen S, Seadawy AR. Propagation of isolated waves of coupled nonlinear (2+1) -dimensional Maccari system in plasma physics. Results Phys 2020;17:102987.